Received: 20 October 2021 | Revised: 31 January 2022 | Accepted: 28 February 2022

DOI: 10.1002/psp4.12785

ARTICLE

Population pharmacokinetics of mobocertinib in healthy volunteers and patients with non–small cell lung cancer

Neeraj Gupta[1] | **Philippe B. Pierrillas**[2] | **Michael J. Hanley**[1] | **Steven Zhang**[1] | **Paul M. Diderichsen**[2]

[1]Takeda Development Center Americas, Inc., Lexington, Massachusetts, USA

[2]Certara USA, Inc., Princeton, New Jersey, USA

Correspondence
Neeraj Gupta, Takeda Development Center Americas, Inc., 95 Hayden Avenue, Lexington, MA 02421, USA.
Email: neeraj.gupta@takeda.com

Funding information
This study was funded by Millennium Pharmaceuticals, Inc., Cambridge, MA, a wholly owned subsidiary of Takeda Pharmaceutical Company Limited.

Abstract

Mobocertinib is an oral tyrosine kinase inhibitor approved for treatment of patients with locally advanced or metastatic non-small cell lung cancer (mNSCLC) with epidermal growth factor receptor gene (*EGFR*) exon 20 insertion mutations whose disease has progressed on or after platinum-based chemotherapy. This population pharmacokinetic (PK) analysis describes the PK of mobocertinib and its active metabolites, AP32960, and AP32914, using data from two phase I studies in healthy volunteers ($n = 110$) and two phase I/II studies in patients with mNSCLC ($n = 317$), including the pivotal phase I/II study. The plasma PK of mobocertinib, AP32960, and AP32914 were well-characterized by a joint semi-mechanistic model that included two compartments for mobocertinib with absorption via three transit compartments, two compartments for AP32960, and one compartment for AP32914. The observed time-dependency in PK was described by an enzyme compartment with drug and metabolite concentration-dependent stimulation of enzyme production, resulting in the enzyme increasing the apparent clearance of mobocertinib, AP32960, and AP32914. Effects of healthy volunteer status (vs. patients with mNSCLC) on apparent oral clearance of all three moieties and on apparent central volume of distribution for mobocertinib were included as structural covariates in the final model. No clinically meaningful differences in mobocertinib PK were observed based on age (18–86 years), race, sex, body weight (37.3–132 kg), mild-to-moderate renal impairment (estimated glomerular filtration rate 30–89 ml/min/1.73 m^2 by modification of diet in renal disease equation), or mild-to-moderate hepatic impairment, suggesting that no dose adjustment is required based on these covariates in patients with mNSCLC.

Study Highlights

WHAT IS THE CURRENT KNOWLEDGE ON THE TOPIC?

Mobocertinib is a first-in-class, oral, irreversible tyrosine kinase inhibitor that demonstrated a favorable benefit–risk profile in patients with metastatic non-small cell lung cancer (mNSCLC) with epidermal growth factor receptor gene

(*EGFR*) exon 20 insertion (ex20ins) mutations in a phase I/II study. Mobocertinib was approved in 2021 for the treatment of platinum-pretreated patients with mNSCLC with *EGFR*ex20ins mutations.

WHAT QUESTION DID THIS STUDY ADDRESS?

This analysis characterized the pharmacokinetics (PK) of mobocertinib and its active metabolites, AP32960 and AP32914, in adult patients with mNSCLC and in healthy volunteers after single- and multiple-dose administration and evaluated the effect of patient-specific covariates on mobocertinib PK.

WHAT DOES THIS STUDY ADD TO OUR KNOWLEDGE?

We developed a joint semimechanistic population PK model that adequately describes the observed PK of mobocertinib and its active metabolites, all of which undergo auto-induction.

HOW MIGHT THIS CHANGE DRUG DISCOVERY, DEVELOPMENT, AND/OR THERAPEUTICS?

The population PK analysis results support dosing recommendations across clinical contexts of use and are reflected in the prescribing information for mobocertinib.

INTRODUCTION

Oncogenic insertion mutations in exon 20 of the epidermal growth factor receptor gene (*EGFR*) occur in 4%–12% of patients with *EGFR*-mutated non-small cell lung cancer (NSCLC)[1–3] and ~2% of all patients with NSCLC.[4] Therapeutic options for patients with metastatic NSCLC (mNSCLC) with *EGFR* exon 20 insertions (*EGFR*ex20ins) are limited. Platinum-based chemotherapy, approved EGFR tyrosine kinase inhibitors (TKIs; e.g., afatinib, erlotinib, and gefitinib), and immune checkpoint inhibitors are associated with a poor prognosis in patients with mNSCLC harboring these rare mutations.[5–10]

Mobocertinib is a first-in-class, potent, oral, irreversible TKI designed to selectively target *EGFR*ex20ins mutations.[11] In preclinical studies, mobocertinib demonstrated selective inhibitory activity against activating *EGFR* mutations, including *EGFR*ex20ins and other *EGFR* mutations (exon 19 deletions and L858R), with or without the T790M resistance mutation.[11] Based on the results of a phase I/II dose-escalation, expansion, and pivotal extension trial (ClinicalTrials.gov NCT02716116),[12] the recommended dose of mobocertinib is 160 mg once daily (q.d.). This dose demonstrated rapid, deep, and durable responses in platinum-pretreated patients with *EGFR*ex20ins-positive mNSCLC, with a confirmed objective response rate (ORR) of 28% per independent review committee (IRC) and 35% per investigators.[13] The median duration of response per IRC was 17.5 months, median progression-free survival per IRC was 7.3 months, and median overall survival was 24.0 months.[13] The safety profile was characterized by manageable gastrointestinal and cutaneous adverse events, consistent with the known profile for EGFR TKIs.[13] Mobocertinib received accelerated approval from the US Food and Drug Administration (FDA) on September 15, 2021, for adult patients with locally advanced or mNSCLC with *EGFR*ex20ins mutations, as detected by an FDA-approved test, whose disease has progressed on or after platinum-based chemotherapy.[14]

Orally administered mobocertinib is systemically absorbed and reaches peak plasma concentration (C_{max}) 4–6 h postdose, with a mean half-life of 20 h after single-dose administration.[15] Mobocertinib is metabolized by cytochrome P450 (CYP3A)-mediated dealkylation to two active metabolites, AP32960 and AP32914, which have approximately equal potency for inhibiting EGFR.[11] The metabolites AP32960 and AP32914, account for 36% and 4% of the combined molar area under the plasma concentration-time curve (AUC), respectively.[14] Mobocertinib is a highly soluble compound with high permeability. Therefore, it exhibits the characteristics of a Biopharmaceutics Classification System Class 1 compound. Following single-dose oral administration of radiolabeled mobocertinib 160 mg, ~76% of the dose was recovered in feces (~6% as unchanged mobocertinib) and 4% in urine (~1% as unchanged mobocertinib).[14] The percentage of the administered dose recovered as AP32960 was ~12% in feces and 1% in urine and as AP32914 was below the lower limit of detection in urine and feces.[14] Overall, this suggests that renal excretion is a minor pathway of drug elimination. In vitro data identified mobocertinib, AP32960, and AP32914 as inhibitors and inducers of CYP3A (data on file, Takeda Development Center Americas). Repeat dosing of mobocertinib 160 mg q.d. in patients with mNSCLC was associated with lower-than-expected accumulation based

on its plasma elimination half-life and the 24-h dosing interval.[16] These observations suggest auto-induction of metabolism by mobocertinib, likely via induction of CYP3A.[16]

Co-administration of mobocertinib with a strong CYP3A inhibitor (itraconazole) increased the molar sum AUC from time zero to infinity ($AUC_{0-\infty}$) of mobocertinib, AP32960, and AP32914 by 527%, whereas co-administration with a strong CYP3A inducer (rifampin) decreased the molar sum of $AUC_{0-\infty}$ by 95%.[16] Food-effect studies showed that there were no clinically meaningful differences in molar sum AUC when mobocertinib was co-administered with a low-fat or high-fat meal compared with fasting conditions.[14,15] Therefore, mobocertinib may be taken with or without food.

In the present study, a joint semimechanistic population pharmacokinetic (PK) model was developed to characterize the plasma PK of mobocertinib and its active metabolites, AP32960 and AP32914, based on available data from phase I/II trials in patients with mNSCLC and phase I trials in healthy volunteers. The final population PK model was used to evaluate potential effects of covariates (e.g., age, sex, race, body weight, eGFR, smoking status, drug product, albumin, alanine aminotransferase [ALT], aspartate aminotransferase [AST], and total bilirubin), to determine if dose adjustments are required based on these patient-specific covariates.

METHODS

Analysis data set

Concentration-time data for mobocertinib and its active metabolites AP32960 and AP32914 were obtained from two phase I studies in healthy adult volunteers and two phase I/II studies in patients with mNSCLC (Table 1). The trials in healthy volunteers evaluated single doses ranging from 20 to 160 mg.[15,16] The phase I/II trial in patients with mNSCLC investigated dose regimens ranging from 5 to 180 mg q.d. and from 40 to 60 mg twice daily.[12] The phase I portion of the phase I/II trial in Japanese patients with mNSCLC evaluated doses of 40, 120, and 160 mg q.d. and only data from the phase I portion of the study were included in the analysis data set. The PK sampling schedule for each trial is listed in Table 1. All studies were performed in accordance with International Council for Harmonization Good Clinical Practice Guidelines; all study protocols were approved by the appropriate institutional review boards and all participants provided written informed consent.

Plasma concentrations of mobocertinib, AP32960, and AP32914 in human plasma were determined by validated liquid chromatography/tandem mass spectrometry (LC-MS/MS)-based assays.[15,16] The lower limit of quantitation (LLOQ) for mobocertinib, AP32960, and AP32914 in plasma was 0.100 ng/ml in both phase I studies[15,16] and in parts 1 and 2 of the global phase I/II study.[12] The LLOQ was 0.250 ng/ml in part 3 of the global phase I/II study and in the Japanese phase I/II study.

A modified M6 method for handling concentrations that were below the LLOQ (BLOQ)[17] was used to optimize the available concentration-time data for the final data set. With this modified method, for all moieties the BLOQ observations occurring before the time to maximum concentration (T_{max}; methodically set at 4 h) were discarded, whereas the first BLOQ observation occurring later than 4 h after dosing was set to LLOQ/2, and subsequent BLOQ samples were discarded. This modification of the original M6 method was made to avoid potential bias that can be introduced by the original M6 method with BLOQ observations occurring during the absorption phase.[18]

Population PK modeling

The population PK analyses were performed using NONMEM (version 7.3.0; ICON Development Solutions[19]) for nonlinear mixed effects models, running under Perl-speaks NONMEM version 4.8.1. Analyses of modeling results and simulations were performed using R version 3.6.0.

A mixed effects population PK model describing the PK of mobocertinib and its metabolites (AP32960 and AP32914) was developed and fitted to observed data, accounting for structural (fixed) effects and interindividual variability (IIV). Initially, a joint linear model was constructed in which oral mobocertinib was absorbed into the parent central compartment and parent drug was either eliminated or metabolized to AP32960 or AP32914, with each metabolite characterized by one-compartment models with linear elimination from the system. Based on available clinical data, the fraction of parent mobocertinib metabolized to AP32960 and AP32914 was set to 62% and 8%, respectively.[16] Two- and three-compartmental models with first-order intercompartmental clearances, as well as more complex models, including transit compartment, and parallel linear and nonlinear elimination mechanisms, were subsequently considered. Mobocertinib and its metabolites were expected to exhibit nonlinear PK due to auto-induction of metabolism via CYP3A.[16] Therefore, the initial linear joint model was extended to include an additional enzyme compartment where the concentration of enzyme increased as plasma concentrations of mobocertinib and/or its metabolites increased. The subsequent enzyme-dependent increase in clearance of mobocertinib

TABLE 1 Summary of studies included in the population PK analysis

Study design	Mobocertinib dosing regimen	PK sampling schedule	*n*[a]
Phase I/II open-label, multicenter, dose-escalation/expansion study in patients with mNSCLC with *EGFR* or *HER2* mutations (NCT02716116)[12]	Part 1 (dose escalation): 5, 10, 20, 40, 80, 120, 160, and 180 mg q.d., and 40 and 60 mg b.i.d. (capsule A or B) Part 2 (expansion; capsule A or B) and Part 3 (extension cohort; capsule C): 160 mg q.d.	Parts 1 and 2: • Cycle 1, day 1: predose, 0.5, 1, 2, 4, 6, 8, and 24 h postdose • Cycle 1, days 8, 15, and 22: predose • Cycle 2, day 1: predose, 0.5, 1, 2, 4, 6, 8, and 24 h postdose • Cycle 3, day 1: predose Part 3: • Cycle 1, day 1: 1–2 h postdose • Cycle 1, day 15: predose and 2–4 h postdose • Cycle 2, day 1: predose and 4–6 h postdose • Cycle 3, day 1: predose and 1–2 h postdose • Cycle 4, day 1: predose and 2–4 h postdose • Cycle 5, day 1: predose and 4–6 h postdose	297
Phase I double-blind, placebo-controlled, single-rising dose study (Part 1) followed by a crossover evaluation of the effects of a low-fat meal on PK (Part 2) and a crossover evaluation of relative bioavailability of 2 capsule drug products (Part 3) in healthy volunteers (NCT03482453)[15]	Part 1: 20, 40, 80, 120, and 160 mg; single dose under fasting conditions (capsule B) Part 2: 120 and 160 mg; single dose with a low-fat meal or under fasting conditions (capsule A) Part 3: 160 mg in 2 capsule drug products (capsule A or B); single dose under fasting conditions	Parts 1 and 2: predose and 0.5, 1, 2, 4, 6, 8, 12, 24, 36, 48, 72, 96, and 168 h postdose Part 3: predose and 0.5, 1, 2, 4, 6, 8, 12, 24, 36, 48, and 72 h postdose	86
Phase I/II, open-label, multicenter, multiple-rising dose study (phase I) with expansion after confirmation of RP2D in adult Japanese patients with mNSCLC (phase II) (NCT03807778) Only data from the phase I part were included in the population PK analysis	Part 1: 40, 120, and 160 mg q.d. (capsule C)	Cycle 1, day 1: predose and 0.5, 1, 2, 4, 6, 8, and 24 h postdose Cycle 1, days 8, 15, and 22: predose Cycle 2, Day 1: predose and 0.5, 1, 2, 4, 6, 8, and 24 h postdose Cycle 3, day 1: predose	20
Phase I, open-label, 2-period, fixed-sequence DDI study with mobocertinib and either a strong CYP3A inhibitor, itraconazole (Part 1) or with a strong CYP3A inducer, rifampin (Part 2) in healthy adult volunteers (NCT03928327).[16] Only data from treatment periods without co-administration with CYP3A modulators were included in the population PK analysis	20 and 160 mg (capsule B and capsule C)	Predose, 0.5, 1, 2, 4, 6, 8, 12, 24, 36, 48, 72, 96, 120, and 168 h postdose	24

Abbreviations: CYP3A, cytochrome P450; DDI, drug–drug interaction; *EGFR*, epidermal growth factor receptor gene; *HER2*, human epidermal growth factor receptor 2; mNSCLC, metastatic non–small cell lung cancer; PK, pharmacokinetic; RP2D, recommended phase II dose.

[a]Number of patients/volunteers included in the population PK analysis data set.

and/or its metabolites was evaluated for its ability to explain the observed nonlinearities in PK.

Pharmacokinetic parameters were estimated using the first-order conditional estimation approximation method without interaction and a "log-transform both sides" approach. Each evaluated model included a variance component characterizing IIV in model parameters that was implemented by exponential random effect models of log-normally distributed individual parameters. Residual unexplained variability was described by an additive (on

the log-scale) error model. In a joint model, the residual error was sampled from a diagonal multivariate normal distribution.

Covariate model development

Covariates evaluated for possible effects on PK parameters are shown in Table 2. Covariates were tested for significance using the stepwise covariate model building tool of Perl-speaks-NONMEM.[20] A multivariate covariate evaluation was carried out with covariates that were significant ($p \leq 0.01$) as univariates. Covariates were retained in the multivariate covariate model if the reduction in the objective function value (OFV) was greater than or equal to 6.64 ($p < 0.01$; degree of freedom [df] = 1) in the forward addition step, and greater than or equal to 10.83 ($p < 0.001$; df = 1) in the backward elimination step. Covariates that did not lead to at least a 5% reduction in IIV were considered for exclusion from the covariate model.[21,22] Continuous covariates were evaluated as power functions and categorical covariates were evaluated as linear relative effects, as exemplified in the following equation:

$$\theta_{TV,i} = \theta_{TV,Pop} \cdot \left(\frac{x_{Cont,i}}{\text{median}\ (x_{Cont,i})} \right)^{\theta_1} \cdot (1 + x_{Cat,i} \cdot \theta_2)$$

where $\theta_{TV,i}$ is the typical parameter for subject i, defined as a function of the typical value for the population, $\theta_{TV,Pop}$, and the individual contributions from continuous (x_{Cont}), and binary categorical (x_{Cat}) covariates, and θ_1 and θ_2 represent the respective covariate coefficients.

Model evaluation

The performance of the final population PK model was evaluated by stratified prediction-corrected visual predictive checks, where the model was simulated with 500 replicates and percentiles (median, and 5th and 95th percentiles) of observed data were compared with the simulated data.[23] Model robustness and parameter estimates were evaluated by 1000 bootstrap replicates stratified by patient status.

Model-based simulations

The exposure metric, AUC from time 0 to 24 h postdose ($AUC_{24\ h}$), was derived as the sum of the molar concentrations of mobocertinib, AP32960, and AP32914 at cycle

TABLE 2 Summary of baseline covariates for the population PK analysis data set

Covariates	(n = 427)
Continuous covariates, mean (SD)	
Age, y	52.9 (17.0)
Body weight, kg	70.4 (15.9)
Albumin, g/L	41.2 (20.7)
AST, U/L	23.7 (12.9)
ALT, U/L	21.8 (15.9)
Bilirubin, μmol/L	9.50 (4.68)
eGFR per MDRD equation, ml/min/1.73 m^2	92.7 (26.7)
Categorical covariates, n (%)	
Sex	
Male	183 (42.9)
Female	244 (57.1)
Race	
White	283 (66.3)
Asian	115 (26.9)
Black	19 (4.4)
American Indian/Alaskan native	1 (0.2)
Other/multiple	9 (2.1)
Mutation status	
EGFR mutation	181 (42.4)
HER2 mutation	36 (8.4)
EGFR/HER2 mutation	4 (0.9)
None or other	206 (48.2)
Smoking status	
Never	320 (74.9)
Former	103 (24.1)
Current	3 (0.7)
Unknown	1 (0.2)
Patient status	
Patient	317 (74.2)
Healthy volunteer	110 (25.8)
Mobocertinib drug product	
Capsules A/B	299 (70.0)
Capsule C	128 (30.0)
Prior treatment	
Patient with mNSCLC with no prior treatment	28 (6.6)
Patient with NSCLC with ≥1 prior treatment	289 (67.7)
Healthy volunteer	110 (25.8)

Abbreviations: ALT, alanine aminotransferase; AST, aspartate aminotransferase; eGFR, estimated glomerular filtration rate; *EGFR*, epidermal growth factor receptor gene; *HER2*, human epidermal growth factor receptor 2; MDRD, modification of diet in renal disease; mNSCLC, metastatic non-small cell lung cancer; NSCLC, non-small cell lung cancer; PK, pharmacokinetic; SD, standard deviation.

one on day 1 and cycle two on day 1 based on the simulated concentration-time profiles, assuming continuous once-daily administration of 160 mg mobocertinib. The correlation between covariates and exposure was evaluated using linear regression of $AUC_{24\,h}$ versus covariates of interest. In addition, the simulated concentration-time profiles were subsequently used to derive the elimination half-life for mobocertinib, AP32960, and AP32914, based on a noncompartmental analysis.

Model-based assessment of the relative bioavailability of three drug-in-capsule drug products

An adapted version of the final population PK model was also applied using a model-based approach[24] to assess the relative bioavailability of mobocertinib, AP32960, and AP32914 when administered as three drug-in-capsule drug products (designated as capsule A, capsule B, and capsule C). First, the relative bioavailability of capsule B versus capsule A was compared using data from the two phase I studies in healthy adult volunteers (Table 1), as these were the only studies in which this specific drug product information was available. For this relative bioavailability assessment, the population PK model was adapted by fixing the enzyme parameters and apparent volume of distribution of the major metabolite (AP32960) to the final model estimates. After comparing the relative bioavailability of capsule B versus capsule A, the relative bioavailability of capsule C versus capsule A/B (combined) was assessed based on the full population PK analysis data set and the final population PK model.

Using the structure of the final population PK model, data were refitted with additional drug product-specific parameters estimated for absorption parameters (absorption rate constant [K_a] and bioavailability [F]) to capture any potential effect of the drug product on the rate and extent of absorption. The parameterization used in the approach is shown in the following equations:

$$K_a = K_{a\,\text{formulation reference}} \cdot \left(1 + \text{Effect}_{\text{formulation test on } K_a}\right) \cdot e^{\eta K_a}$$

$$F = F_{\text{formulation reference}} \cdot \left(1 + \text{Effect}_{\text{formulation test on } F}\right)$$

$$\text{Effect formulation} = 0 \text{ for the reference formulation}$$

For the refitted models, the assessment of relative bioavailability was based on both a comparison of model parameters and on a comparison of exposure metrics. Bioequivalence was concluded if the 90% confidence interval (CI) ratio of parameter values for the test drug product versus the reference drug product was included in the 80% to 125% range for both the K_a and the F. For the comparison of exposure metrics, 500 sets of parameter values were sampled from the variance–covariance matrix of the estimate of the refitted model, and $AUC_{24\,h}$ and C_{max} were derived from the simulations at cycle one on day 1 and cycle two on day 1. The ratio of simulated PK metrics and associated 90% CIs were computed and bioequivalence was concluded if the CI fell in the 80% to 125% range.

RESULTS

Data set summary

The population PK analysis data set comprised 427 participants (110 healthy volunteers and 317 patients with mNSCLC) from four clinical studies (Table 1).[12,15,16] Demographics and baseline characteristics of participants included in the final population PK analysis data set are presented in Table 2. The percentage of post-treatment samples that were BLOQ was less than the predefined threshold of 10% in the overall data set. However, the proportion of AP32914 samples that were BLOQ was 14.7%. The number of BLOQ samples and exclusions based on the modified M6 method are summarized by analyte in Appendix S1: Table S1.

Development of the population PK model

An optimal base model for single-dose mobocertinib PK was identified as a two-compartment structural model with absorption of mobocertinib through three transit compartments. Optimal single-dose models for metabolites AP32960 and AP32914 were incorporated as a two-compartment model for AP32960 and a one-compartment model for AP32914. To better describe the multiple-dose PK data, the potential effect of drug-dependent stimulation of CYP3A (i.e., auto-induction of metabolism) was implemented by the addition of an enzyme compartment to the model, where the rate of enzyme production was described by a maximum effect (E_{max}) model parametrized by an E_{max} parameter and a potency parameter (half-maximal effective concentration [EC_{50}]) based on the molar sum of mobocertinib, AP32960, and AP32914 plasma concentrations, and assumed a similar molar potency of the three moieties. The effect of the enzyme compartment was to increase the apparent oral clearance of mobocertinib, AP32960, and AP32914.

An effect of healthy volunteer status on the apparent central volume for mobocertinib and on the apparent oral clearance of all three moieties was included to describe the difference in PK between patients and healthy volunteers.

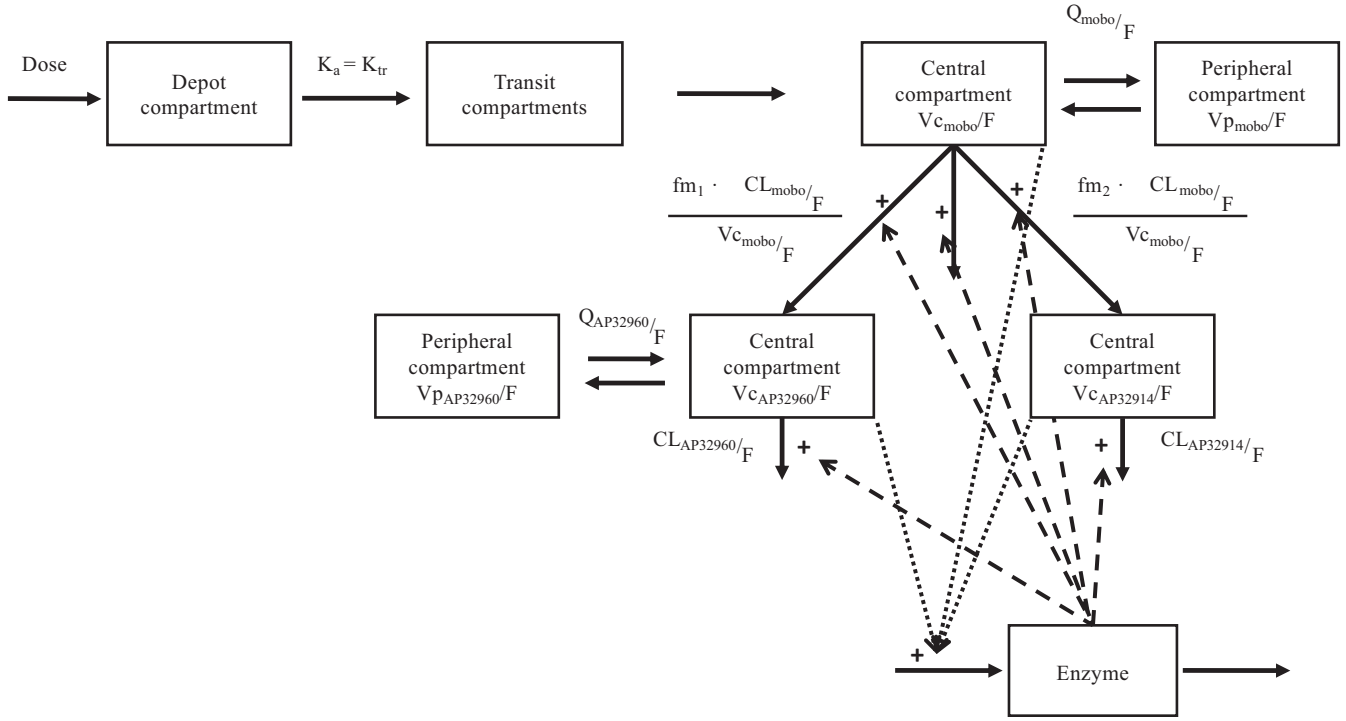

FIGURE 1 Structural model describing the PK of mobocertinib and its active metabolites, AP32960 and AP32914. The enzyme compartment impacted all three elimination pathways from the central compartment for mobocertinib; however, only one dashed arrow is shown for visual simplicity. CL/*F*, apparent oral clearance; *F*, bioavailability; f_m, fraction metabolized; K_a, absorption rate constant; K_{tr}, transit rate constant; mobo, mobocertinib; PK, pharmacokinetic; *Q*/*F*, intercompartmental clearance; Vc/*F*, apparent central volume of distribution; Vp/*F*, apparent peripheral volume of distribution

However, no additional significant covariates were identified during univariate covariate screening. During subsequent model refinement steps, a correlation between multiple subject-level random effects (ETAs) became evident, and was included in the model between apparent central volume of distribution of mobocertinib (Vc_{mobo}/F), apparent oral clearance of mobocertinib (CL_{mobo}/F), AP32960 ($CL_{AP32960}/F$), and AP32914 ($CL_{AP32914}/F$). This was addressed by estimation of covariance in CL_{mobo}/F, Vc_{mobo}/F, $CL_{AP32960}/F$, and $CL_{AP32914}/F$, which led to a significant drop in the OFV ($p < 0.0001$). The resulting final population PK model provided a joint description of mobocertinib, AP32960, and AP32914 plasma concentrations as shown in Figure 1. Parameter estimates for the final population PK model are presented in Table 3.

Population PK model evaluation

Plots of observed concentrations versus population-predicted (Figure 2a) and individual-predicted concentrations (Figure 2b) and plots of conditional weighted residual (CWRES) values versus time (Figure 2c) and predicted concentrations (Figure 2d) indicated that the final population PK model adequately described the observed PK data. Plots of observed versus predicted concentrations of mobocertinib, AP32960, and AP32914 over time are shown in Appendix S1: Figure S1. Distributions of ETAs were centered on zero and were approximately normally distributed (Appendix S1: Figure S2). In addition, the final model parameters (Table 3) were contained within the 95% CI determined by a bootstrap analysis, with 997 of 1000 replicates achieving successful convergence. Prediction-corrected visual predictive checks in patients with mNSCLC indicated that the model was able to adequately predict the median and 95% CI values for observed concentrations with good accuracy (Figure 3). Based on derivation of PK parameters from the final population PK model, the geometric mean (percent coefficient of variation [%CV]) apparent volume of distribution at steady state (Vss/*F*) for mobocertinib was 3509 L (38%). The estimated EC_{50} value for the enzyme compartment (213 nM) was similar to the typical C_{max} of the molar sum at steady-state following administration of 160 mg q.d. mobocertinib (214 nM).

Model-based simulations

The final population PK model was then used to simulate the mobocertinib, AP32960, and AP32914

TABLE 3 Parameter estimates based on the final population PK model

Parameter	Estimate	RSE (%)	Shrinkage (%)	Untransformed parameter	Bootstrap 95% CI
Population parameter					
K_a	0.752[a]	3.29	–	2.12 h^{-1}	2.02–2.23
Vc_{mobo}/F	7.76[a]	0.418	–	2340 L	2200–2500
CL_{mobo}/F	4.68[a]	0.928	–	108 L/h	95.2–116
Q_{mobo}/F	2.46[a]	12.6	–	11.7 L/h	6.6–25.4
Vp_{mobo}/F	7.01	1.68	–	1110 L	888–1440
$CL_{AP32960}/F$	4.76[a]	0.834	–	117 L/h	103–124
$Vc_{AP32960}/F$	2.55[a]	4.23	–	12.8 L	9.9–15.1
$Q_{AP32960}/F$	3.28[a]	1.31	–	26.5 L/h	23.7–28.4
$Vp_{AP32960}/F$	6.99	1.12	–	1090 L	914–1240
$CL_{AP32914}/F$	4.82[a]	0.901	–	124 L/h	109–134
$Vc_{AP32914}/F$	3.42[a]	2.06	–	30.6 L	25.7–34.2
HV on Vc_{mobo}/F	0.787	12.7	–	0.787	0.591–0.987
HV on CL_{mobo}/F	0.900	15.0	–	0.900	0.680–1.28
HV on $CL_{AP32960}/F$	0.738	13.0	–	0.738	0.581–1.00
HV on $CL_{AP32914}/F$	0.909	15.0	–	0.909	0.676–1.27
K_{enz}	−5.54[a]	3.26	–	0.00392 h^{-1}	0.00272–0.00673
EC_{50}	−1.55[a]	39.6	–	213 nM	16.9–225,000
E_{max}	0.781	44.9	–	0.781	0.301–417
IIV					
IIV K_a	0.209	10.5	3.43	45.7%	41.6–50.7
IIV Vc_{mobo}/F	0.237	9.97	6.88	48.7%	44.0–53.6
IIV CL_{mobo}/F	0.246	8.36	2.92	49.6%	45.2–53.8
Cov: CL_{mobo}/F and Vc_{mobo}/F	0.197	9.12	–	0.814	0.161–0.235
IIV $CL_{AP32960}/F$	0.157	9.85	3.69	39.6%	35.7–43.8
Cov: $CL_{AP32960}/F$ and Vc_{mobo}/F	0.153	9.62	–	0.794	0.125–0.188
Cov: $CL_{AP32960}/F$ and CL_{mobo}/F	0.182	9.35	–	0.927	0.149–0.220
IIV $CL_{AP32914}/F$	0.295	7.93	3.23	54.3%	49.7–58.5
Cov: $CL_{AP32914}/F$ and Vc_{mobo}/F	0.194	9.98	–	0.735	0.157–0.235
Cov: $CL_{AP32914}/F$ and CL_{mobo}/F	0.221	8.79	–	0.821	0.181–0.262
Cov: $CL_{AP32914}/F$ and $CL_{AP32960}/F$	0.171	9.85	–	0.797	0.138–0.210
Residual variability, additive error on log scale					
Mobocertinib	0.414	3.20	5.07	41.4%	0.389–0.441
AP32960	0.373	4.28	5.03	37.3%	0.344–0.405
AP32914	0.405	3.23	5.55	40.5%	0.379–0.431

Note: The 95% CIs were generated from a bootstrap run of 1000 replicated data sets. The 95% CIs show untransformed parameters, except for covariance parameters, where 95% CIs are on the scale of the parameter estimate.

Abbreviations: CI, confidence interval derived from bootstrap; CL/*F*, apparent oral clearance; Cov, covariance; EC_{50}, concentration at 50% maximal induction effect; E_{max}, maximal induction effect; HV, healthy volunteer; IIV, interindividual variability; K_a, absorption rate constant; K_{enz}, rate constant for enzyme synthesis/degradation; mobo, mobocertinib; PK, pharmacokinetic; *Q*/*F*, apparent intercompartmental clearance; RSE, relative standard error; Vc/*F*, apparent central volume of distribution; Vp/*F*, apparent peripheral volume of distribution.

[a]Parameter estimated on a log scale.

concentration-time profiles and derive $AUC_{24\,h}$ values for all individuals in the analysis data set, assuming continuous once-daily administration of mobocertinib 160 mg, to evaluate the correlation between individual-predicted exposure and covariates of interest. Based on these simulations, the geometric mean (%CV) elimination

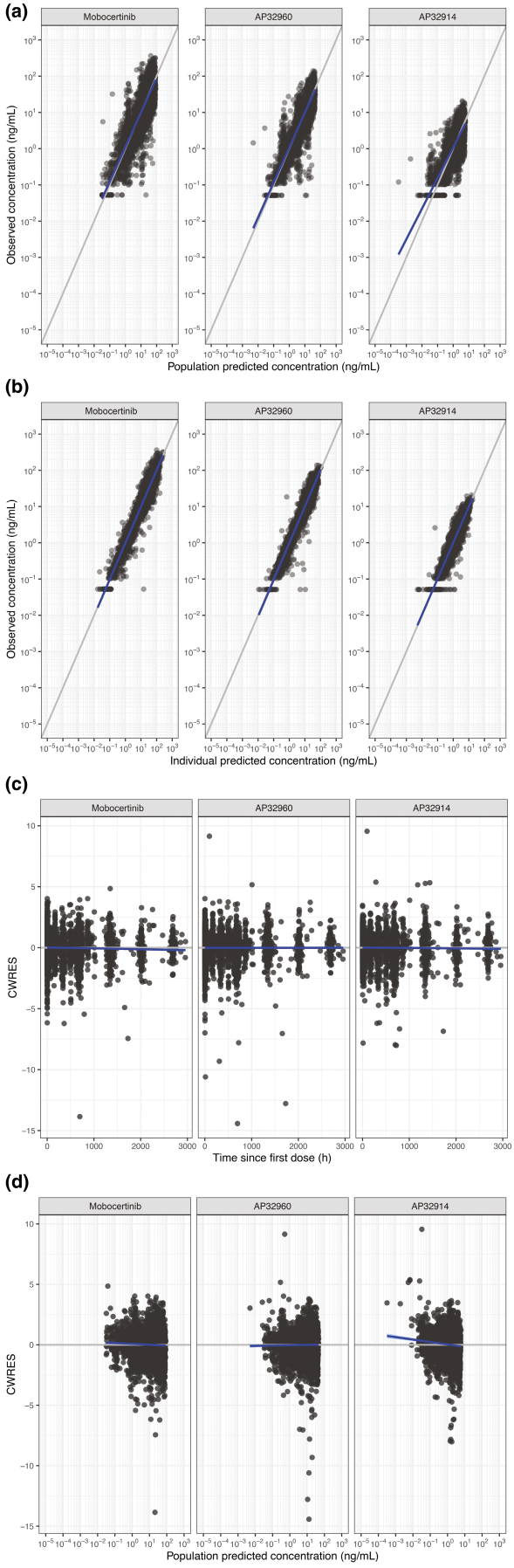

FIGURE 2 Observed concentrations of mobocertinib, AP32960, and AP32914 versus (a) population-predicted concentrations and (b) individual-predicted concentrations from the final population pharmacokinetic (PK) model. Conditional weighted residuals (CWRES) versus (c) time after first dose and (d) population-predicted values from the final population PK model. Dots represent individual data points, solid blue lines represent linear regression lines, and gray lines represent lines of identity

half-lives for mobocertinib, AP32960, and AP32914 at steady-state were 18 h (21%), 24 h (20%), and 18 h (21%), respectively, in patients with cancer. The simulations confirmed the covariate effect of patient status identified in the model and demonstrated that the estimated mean $AUC_{24\ h}$ (based on the sum of molar concentrations of mobocertinib, AP32960, and AP32914) was 43.1% lower in healthy volunteers than in patients with mNSCLC at cycle two on day 1 (Figure 4a). For continuous covariates (age, body weight, eGFR, ALT, AST, total bilirubin, and albumin), the magnitudes of the percentage difference in $AUC_{24\ h}$ in patients with mNSCLC at the 5th and 95th percentiles of these covariate values relative to the $AUC_{24\ h}$ at the median of individual covariate values were at most 12% (Figure 4b). For categorical covariates (sex, race, smoking status, and drug product), the difference in mean $AUC_{24\ h}$ in patients with mNSCLC was at most 5% across categories. These observed differences in $AUC_{24\ h}$ were well below the variability in $AUC_{24\ h}$ observed across the entire analysis population, where the 5th and 95th percentiles were −47% to 191% relative to the median $AUC_{24\ h}$. Accordingly, these covariates have no clinically meaningful effect on systemic exposures of mobocertinib, AP32960, and AP32914.

Relative bioavailability of three drug-in-capsule drug products

The intended commercial product of mobocertinib, as well as the drug product used in clinical studies, is an immediate-release capsule, in which the drug substance is filled directly into hard gelatin capsules with no excipients. Three processes were used during development to manufacture the mobocertinib drug substance, resulting in three drug products being administered in clinical studies (designated as capsule A, capsule B, and capsule C). Therefore, it was of interest to assess the relative bioavailability of the three drug products by adapting the final population PK model by incorporating drug product specific parameters.

Because a dedicated relative bioavailability study demonstrated that capsule A and capsule B were bioequivalent,[15] the model-based relative bioavailability

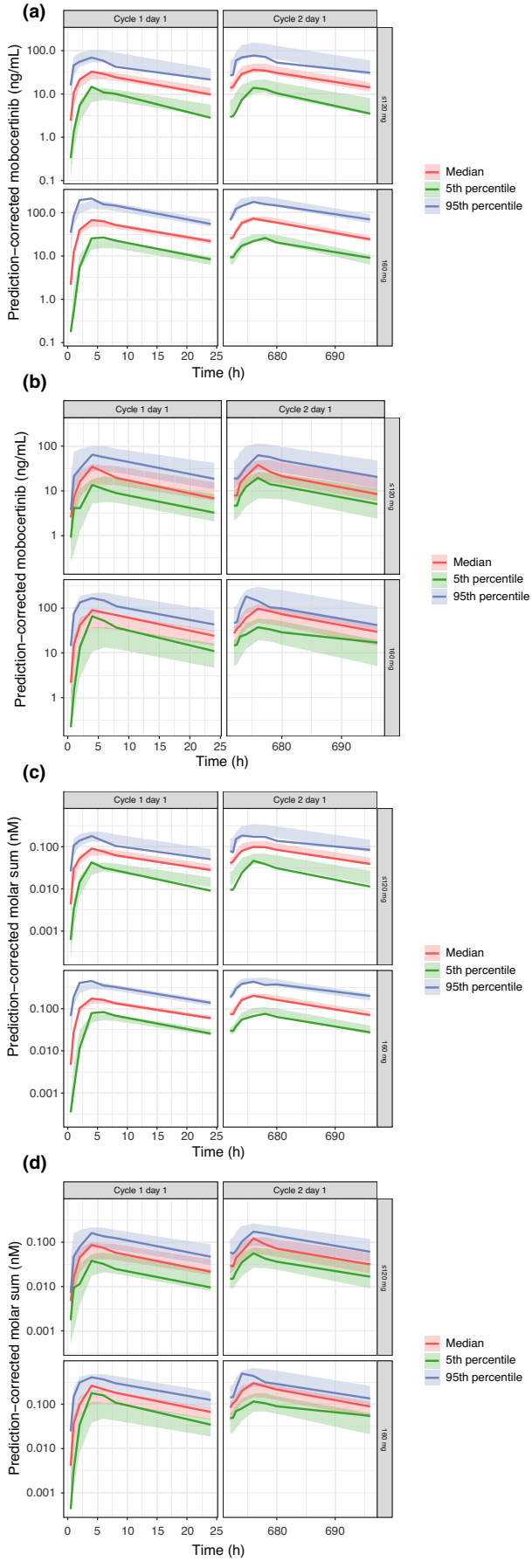

FIGURE 3 Prediction-corrected visual predictive checks of the final population PK model showing mobocertinib plasma concentrations in patients with mNSCLC in (a) the global phase I/II study and (b) in the Japanese phase I/II study, and showing molar sum plasma concentrations of mobocertinib, AP32960, and AP32914 in patients with mNSCLC in (c) the global phase I/II study and (d) in the Japanese phase I/II study. The top graphs in each panel show data for mobocertinib doses greater than or equal to 120 mg and the bottom graphs show data for the 160-mg dose. The red solid line represents the observed median; green and blue solid lines represent observed 5th and 95th percentiles. The red area represents the 95% CI of the simulated median, and green and blue areas represent the 95% CIs of the simulated 5th and 95th percentiles. Only bins with more than four observations greater than the lower limit of quantification are displayed. CI, confidence interval; mNSCLC, metastatic non-small cell lung cancer; NSCLC, non-small cell lung cancer; PK, pharmacokinetic

assessment initially evaluated the relative bioavailability of these two drug products using data from the two studies in healthy volunteers as a means to assess the ability of the model-based approach to confirm the bioequivalence of these two drug products. The adapted population PK model provided an adequate description of the observed data in healthy volunteers (Appendix S1: Figure S3). The 90% CI for the effect of capsule B on K_a and F included zero, indicating that the capsule effect on these parameters was not significantly different from zero (Appendix S1: Table S2). The 90% CIs for the capsule B/capsule A ratio for model-estimated values of K_a (107%, 90% CI: 95%–118%) and F (103%, 90% CI: 86%–120%) were contained completely within the 80%–125% bioequivalence range. There were no significant differences in simulated PK exposure metrics ($AUC_{24\ h}$ and C_{max}) for mobocertinib, AP32960, AP32914, and molar sum concentrations of the three analytes between capsule B and capsule A in healthy volunteers (Appendix S1: Table S3). Thus, the model-based relative bioavailability assessments were consistent with bioequivalence between capsule A and capsule B.

Because no differences in mobocertinib PK were observed between capsule A and capsule B, data from participants who received capsule A and/or B were then pooled for comparison to capsule C using the full population PK analysis data set. The adapted model provided an adequate description of the full data set (Appendix S1: Figure S4). Capsule C did not have a significant effect on model-estimated K_a or F (Appendix S1: Table S4) or simulated exposure metrics ($AUC_{24\ h}$ and C_{max}; Appendix S1: Table S5). The test/reference ratio for capsule C versus capsule A/B for the model-estimated values of K_a (94.8%, 90% CI: 89.4%–100%) and F (109%, 90% CI: 99.7%–118%) were

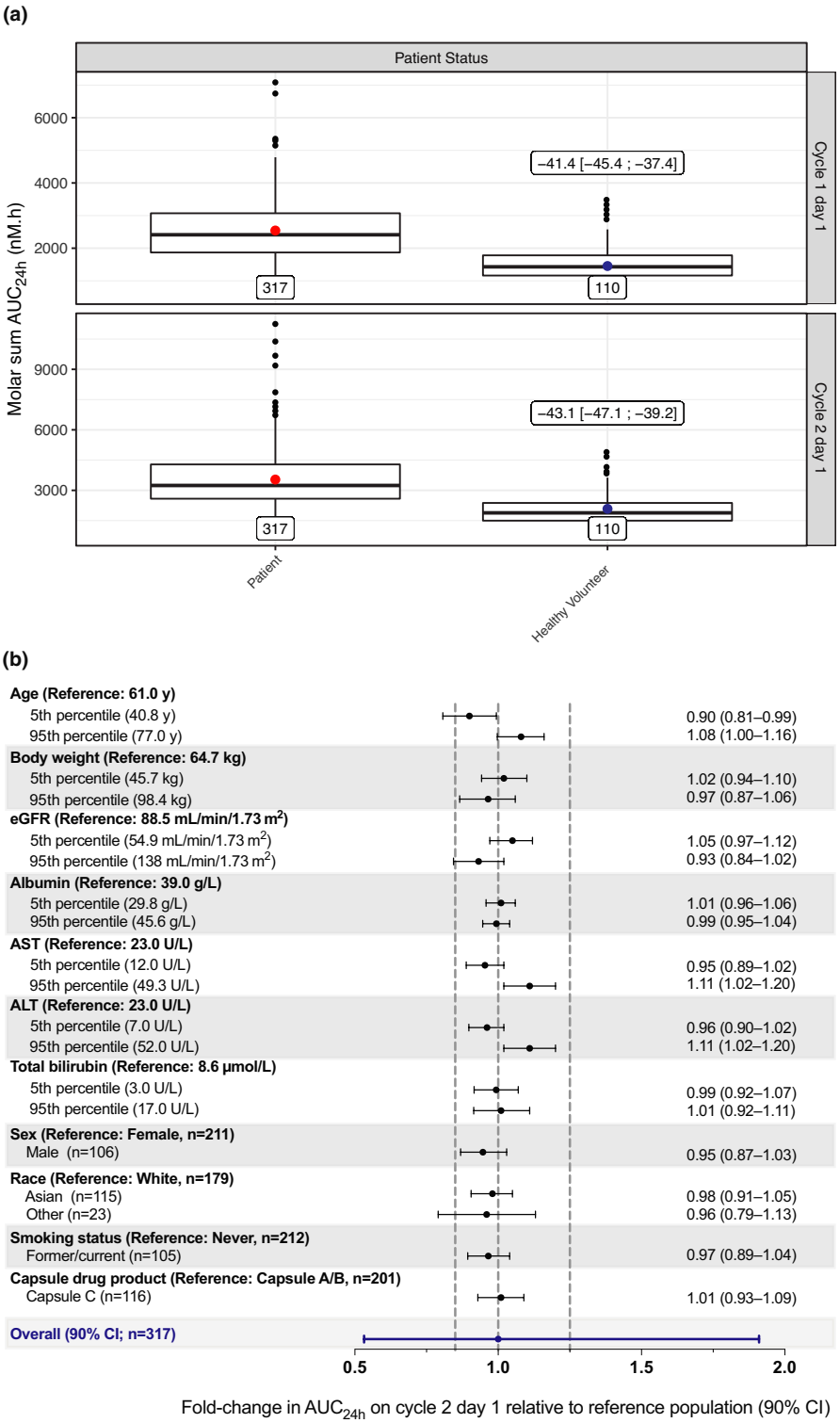

FIGURE 4 (a) Individual-predicted molar sum exposure ($AUC_{24\,h}$) after administration of mobocertinib 160 mg once daily (cycle 2, day 1) stratified by patient status. Red and blue dots represent means. Numbers (brackets) at the top of plots show the percentage change in mean $AUC_{24\,h}$ (with 95% CI) in the healthy volunteer category relative to the patient category, whereas numbers at the bottom of the plots show the number of individuals in each category. (b) Individual-predicted relative molar sum exposure following daily dosing of mobocertinib 160 mg in the patient population based on the final population PK model stratified by covariates of interest. For categorical covariates, the ratio of exposure for the category versus the reference category is shown. For continuous covariates, the ratios of exposure for the 5th and 95th percentiles of the covariate versus the median are shown. The blue bar illustrates the 5th to 95th percentile exposure range across the entire patient population. ALT, alanine aminotransferase; AST, aspartate aminotransferase; $AUC_{24\,h}$, area under the concentration-time curve from time 0 to 24 h postdose; CI, confidence interval; eGFR, estimated glomerular filtration rate calculated using the modification of diet in renal disease (MDRD) formula; PK, pharmacokinetic

contained completely within the 80%–125% bioequivalence range. As a result, the model-based relative bioavailability assessment results support the conclusion that the three mobocertinib drug products are bioequivalent and therefore provide similar systemic exposures after single- and multiple-dose administration.

DISCUSSION

This population PK analysis used data from four clinical studies to develop a population PK model that jointly described the plasma PK of mobocertinib and its two active metabolites, AP32960 and AP32914. In our joint

model, mobocertinib PK were well-characterized by a two-compartment model with absorption described by a first-order process through three transit compartments. The formation of AP32960 and AP32914 was dependent on mobocertinib metabolism, and the PK of AP32960 were best described by a two-compartment model, whereas the PK of AP32914 were adequately described by a one-compartment model. Mobocertinib and its metabolites were expected to exhibit nonstationary, time-dependent PK based on in vitro data indicating that mobocertinib, AP32960, and AP32914 are both substrates and inducers of CYP3A.[11] Therefore, an additional enzyme compartment was included in the population PK model, where the production of enzyme was described by an E_{max} model based on the molar sum concentration of mobocertinib, AP32960, and AP32914, assuming similar molar potency of the three moieties. The effect of the enzyme compartment was to increase the apparent clearance of mobocertinib, AP32960, and AP32914. The estimated rate constant for the enzyme compartment (K_{enz}, 0.00392 h^{-1}) was generally consistent with that reported for the known CYP3A inducer rifampicin (0.00603 h^{-1}).[25] Similar models have been used to successfully describe the PK of other drugs that undergo enzymatic auto-induction, including lorlatinib[26] and molibresib.[27]

Observed PK differences between healthy volunteers and patients with mNSCLC were described in the population PK model by including corresponding covariate effects on the central volume of distribution for mobocertinib and on the apparent oral clearance parameters for mobocertinib, AP32960, and AP32914. Inclusion of these covariate effects predicted a 43.1% lower molar sum exposure at steady-state in healthy volunteers compared with patients. The difference between healthy volunteers and patients with cancer may, in part, be attributable to the lack of multiple-dose data in healthy volunteers. Additionally, cancer-induced inflammation may alter the expression and activity of CYP enzymes, potentially contributing to differences in drug metabolism between healthy volunteers and patients with cancer.[28]

Covariates of clinical interest, including age, body weight, race, sex, patient status (patient with mNSCLC vs. healthy volunteer), smoking status, capsule drug product, albumin, ALT, AST, bilirubin, and eGFR were evaluated as predictors of inter-individual variability. Except for patient status, none of these covariates significantly improved model fit while simultaneously reducing unexplained between-subject variability by at least 5%. Furthermore, based on correlations between covariate values and individual-predicted exposures, none of these covariates had clinically meaningful effects on systemic exposures of combined molar mobocertinib, AP32960, and AP32914 in patients with mNSCLC, indicating that dose adjustments are not required based on these covariates, as reflected in the prescribing information.[14]

The final population PK model was subsequently adapted to establish bioequivalence among three different capsule drug products of mobocertinib, which supported the integration of relevant safety and efficacy data from studies that administered capsules A, B, and/or C. Specifically, adaptation of the final model demonstrated that capsules A, B, and C did not differ in absorption or exposure parameters and are bioequivalent after single- and multiple-dose administration. Thus, capsules A, B, and C are expected to provide similar systemic exposures of mobocertinib, AP32960, and AP32914. The establishment of bioequivalence using a model-based approach obviated the need for a dedicated clinical study comparing the drug products.

CONCLUSIONS

In conclusion, a joint-population PK model was developed to characterize the PK of mobocertinib and its active metabolites, AP32960 and AP32914, after single- and multiple-dose administration. An enzyme compartment model was used to adequately describe the observed time-dependency in PK. Covariates of clinical interest, including age, sex, body weight, race, mild-to-moderate renal impairment, and mild hepatic impairment, did not have a clinically meaningful effect on mobocertinib PK. Thus, no dose adjustment is needed based on these covariates, as described in the US Prescribing Information for mobocertinib.

ACKNOWLEDGEMENTS

The authors would like to thank the patients, their families, and their caregivers; the study investigators and their team members at each study site; and colleagues from Millennium Pharmaceuticals, Inc., Cambridge, MA, a wholly owned subsidiary of Takeda Pharmaceutical Company Limited. Arne van Schanke, PhD, of Certara, Princeton, NJ, is acknowledged for writing the population PK study report. Teodor G. Paunescu, PhD (Takeda Pharmaceuticals U.S.A., Inc.) is acknowledged for editorial assistance. Professional medical writing assistance was provided by Lela Creutz, PhD, formerly of Peloton Advantage, LLC, an OPEN Health company, Parsippany, NJ, and funded by Millennium Pharmaceuticals, Inc.

CONFLICT OF INTEREST

Neeraj Gupta is employed by Takeda; Philippe B. Pierrillas is employed by Certara and is a consultant for Takeda; Michael J. Hanley is employed by Takeda; Steven Zhang is employed by Takeda; Paul M.

Diderichsen is employed by Certara and is a consultant for Takeda.

AUTHOR CONTRIBUTIONS

M.J.H. and N.G. wrote the manuscript. N.G., M.J.H., and S.Z. designed the research. P.M.D. and P.B.P. performed the research and analyzed the data.

ORCID

Neeraj Gupta https://orcid.org/0000-0002-5500-5218
Philippe B. Pierrillas https://orcid.org/0000-0003-4284-9531
Michael J. Hanley https://orcid.org/0000-0001-9266-2797
Steven Zhang https://orcid.org/0000-0001-6583-6771
Paul M. Diderichsen https://orcid.org/0000-0003-3567-7903

REFERENCES

1. Riess JW, Gandara DR, Frampton GM, et al. Diverse *EGFR* exon 20 insertions and co-occurring molecular alterations identified by comprehensive genomic profiling of NSCLC. *J Thorac Oncol*. 2018;13:1560-1568.
2. Oxnard GR, Lo PC, Nishino M, et al. Natural history and molecular characteristics of lung cancers harboring *EGFR* exon 20 insertions. *J Thorac Oncol*. 2013;8:179-184.
3. Yasuda H, Kobayashi S, Costa DB. *EGFR* exon 20 insertion mutations in non-small-cell lung cancer: preclinical data and clinical implications. *Lancet Oncol*. 2012;13:e23-e31.
4. Fang W, Huang Y, Hong S, et al. EGFR exon 20 insertion mutations and response to osimertinib in non-small-cell lung cancer. *BMC Cancer*. 2019;19:595.
5. O'Kane GM, Bradbury PA, Feld R, et al. Uncommon *EGFR* mutations in advanced non-small cell lung cancer. *Lung Cancer*. 2017;109:137-144.
6. Byeon S, Kim Y, Lim SW, et al. Clinical outcomes of EGFR exon 20 insertion mutations in advanced non-small cell lung cancer in Korea. *Cancer Res Treat*. 2019;51:623-631.
7. Wang Y, Yang G, Li J, et al. Real-world treatment outcome of advanced Chinese NSCLC EGFR exon 20 insertion patients [abstract]. *J Clin Oncol*. 2019;37(15 suppl):9043.
8. Udagawa H, Matsumoto S, Ohe Y, et al. Clinical outcome of non-small cell lung cancer with EGFR/HER2 exon 20 insertions identified in the LC-SCRUM-Japan [abstract OA07.03]. *J Thorac Oncol*. 2019;14(10 suppl):S224.
9. Yang G, Li J, Xu H, et al. *EGFR* exon 20 insertion mutations in Chinese advanced non-small cell lung cancer patients: molecular heterogeneity and treatment outcome from nationwide real-world study. *Lung Cancer*. 2020;145:186-194.
10. Negrao MV, Reuben A, Ponville Robichaux J, et al. Association of EGFR and HER-2 exon 20 mutations with distinct patterns of response to immune checkpoint blockade in non-small cell lung cancer [abstract]. *J Clin Oncol*. 2018;36(15 suppl):9052.
11. Gonzalvez F, Vincent S, Baker TE, et al. Mobocertinib (TAK-788): a targeted inhibitor of *EGFR* exon 20 insertion mutants in non–small cell lung cancer. *Cancer Discov*. 2021;11:1672-1687.
12. Riely GJ, Neal JW, Camidge DR, et al. Activity and safety of mobocertinib (TAK-788) in previously treated non–small cell lung cancer with *EGFR* exon 20 insertion mutations from a phase 1/2 trial. *Cancer Discov*. 2021;11:1688-1699.
13. Zhou C, Ramalingam SS, Kim TM, et al. Treatment outcomes and safety of mobocertinib in platinum-pretreated patients with *EGFR* exon 20 insertion–positive metastatic non–small cell lung cancer: a phase 1/2 open-label nonrandomized clinical trial. *JAMA Oncol*. 2021;7(12):e214761.
14. Takeda Pharmaceuticals America, Inc. *Exkivity (mobocertinib) [package insert]*. Takeda Pharmaceuticals America, Inc; 2021.
15. Zhang S, Jin S, Griffin C, et al. Single-dose pharmacokinetics and tolerability of the oral epidermal growth factor receptor inhibitor mobocertinib (TAK-788) in healthy volunteers: low-fat meal effect and relative bioavailability of 2 capsule products. *Clin Pharmacol Drug Dev*. 2021;10:1028-1043.
16. Zhang S, Jin S, Griffin C, et al. Effects of itraconazole and rifampin on the pharmacokinetics of mobocertinib (TAK-788), an oral epidermal growth factor receptor inhibitor, in healthy volunteers. *Clin Pharmacol Drug Develop*. 2021;10:1044-1053.
17. Beal SL. Ways to fit a PK model with some data below the quantification limit. *J Pharmacokinet Pharmacodyn*. 2001;28:481-504.
18. Bergstrand M, Karlsson MO. Handling data below the limit of quantification in mixed effect models. *AAPS J*. 2009;11:371-380.
19. Bauer RJ. *NONMEM Users Guide: Introduction to NONMEM 7.3.0*. ICON Development Solutions; 2015.
20. Wahlby U, Jonsson EN, Karlsson MO. Comparison of stepwise covariate model building strategies in population pharmacokinetic-pharmacodynamic analysis. *AAPS PharmSci*. 2002;4:E27-E79.
21. Gupta N, Diderichsen PM, Hanley MJ, et al. Population pharmacokinetic analysis of ixazomib, an oral proteasome inhibitor, including data from the phase III TOURMALINE-MM1 study to inform labelling. *Clin Pharmacokinet*. 2017;56:1355-1368.
22. Gupta N, Wang X, Offman E, et al. Population pharmacokinetics of brigatinib in healthy volunteers and patients with cancer. *Clin Pharmacokinet*. 2021;60:235-247.
23. Bergstrand M, Hooker AC, Wallin JE, Karlsson MO. Prediction-corrected visual predictive checks for diagnosing nonlinear mixed-effects models. *AAPS J*. 2011;13:143-151.
24. Seng Yue C, Ozdin D, Selber-Hnatiw S, Ducharme MP. Opportunities and challenges related to the implementation of model-based bioequivalence criteria. *Clin Pharmacol Ther*. 2019;105:350-362.
25. Svensson RJ, Aarnoutse RE, Diacon AH, et al. A population pharmacokinetic model incorporating saturable pharmacokinetics and autoinduction for high rifampicin doses. *Clin Pharmacol Ther*. 2018;103:674-683.
26. Chen J, Houk B, Pithavala YK, Ruiz-Garcia A. Population pharmacokinetic model with time-varying clearance for lorlatinib using pooled data from patients with non-small cell lung cancer and healthy participants. *CPT Pharmacometrics Syst Pharmacol*. 2021;10:148-160.
27. Krishnatry AS, Voelkner A, Dhar A, Prohn M, Ferron-Brady G. Population pharmacokinetic modeling of molibresib and its active metabolites in patients with solid tumors: a semi-mechanistic autoinduction model. *CPT Pharmacometrics Syst Pharmacol*. 2021;10:709-722.

28. Coutant DE, Kulanthaivel P, Turner PK, et al. Understanding disease-drug interactions in cancer patients: implications for dosing within the therapeutic window. *Clin Pharmacol Ther*. 2015;98:76-86.

SUPPORTING INFORMATION

Additional supporting information may be found in the online version of the article at the publisher's website.

How to cite this article: Gupta N, Pierrillas PB, Hanley MJ, Zhang S, Diderichsen PM. Population pharmacokinetics of mobocertinib in healthy volunteers and patients with non–small cell lung cancer. *CPT Pharmacometrics Syst Pharmacol*. 2022;11:731-744. doi:10.1002/psp4.12785